24th COBEM - 2017

24th ABCM International Congress of Mechanical Engineering
December 3-8, 2017, Curitiba, PR, Brazil

COBEM-2017-0352
THERMAL CHARACTERIZATION OF HARDMETAL BY OPEN PHOTOACOUSTIC CELL TECHNIQUE

Juliana Soares de Souza
Regiane Gordia Drabeski
Programa de Pós Graduação em Engenharia Mecânica, Federal University of Technology - Paraná, Ponta Grossa, PR 84016-210, Brazil
julianasdesouza@gmail.com,
regianedrabeski@gmail.com

Aldo Braghini Junior
Programa de Pós Graduação em Engenharia Mecânica, Federal University of Technology - Paraná, Ponta Grossa, PR 84016-210, Brazil
aldo@utfpr.edu.br

Daniele Toniolo Dias
Programa de Pós Graduação em Engenharia Mecânica, Federal University of Technology - Paraná, Ponta Grossa, PR 84016-210, Brazil
danieletdias@utfpr.edu.br

Abstract. *In the present work, the open photoacoustic cell technique was used to measure the thermal diffusivity of commercial hardmetal used as metal-cutting tool in the process called dry machining. This is of great importance, because the metal cutting tool requires good thermal properties due to the tool flank wear – abrasion and friction. The inserts from different manufacturers both used in milling of steel were named X and Y. The average value found for the X and Y samples were* $\approx(19.4 \pm 0.7) \times 10^{-6}$ m^2/s *and* $\approx(26.3 \pm 0.9) \times 10^{-6}$ m^2/s *respectively. These results agree with the values of the literatures where same and other techniques have been employed for several sintered WC/Co hardmetal. In addition, the microstructural characterization of samples was done by X-ray diffraction and scanning electron microscopy.*

Keywords: *cutting tools, XRD, SEM*

1. INTRODUCTION

The metallurgical cutting industries have been strongly seeking materials that exhibit characteristics such as low-cost, reliability, mechanical strength, high hardness and good thermal behavior. Cemented carbides are materials that have such characteristics, and hardmetal (cemented carbide) is an example of this type of material. A hardmetal alloy is a composite material whose properties depend on the constituents combination (WC and Co), which are manipulated in such a way as to get the required characteristics (Su, *et al.*, 2016). In its simplest form, the cemented carbide consists of WC as hard phase and Co as cementing binder phase. The conventional production route is through powder metallurgy (Karimi, *et al.*, 2017)

Hardmetal is one of the most important materials used in the manufacture of cutting tools (Davim, 2011). Due to high competitiveness and the demand for a more sustainable machining with minimal environmental impact, the searches for reduction or elimination of cutting fluids usage has increased. This process is called dry machining. However, the disadvantage of this process is of the heat generated during the material removal, which would be dispelled if there were the cut fluid presence, directly affecting the wear cutting tools.

The fundamental properties of the hardmetal are hardness, both at room temperature and high temperature, wear resistance that depends directly on hardness and fracture toughness (Myalska, *et al.*, 2017). The thermal characterization is a preponderant factor in the analysis of this type of material, since the hardmetal is used in situations of great frictional wear, which makes the control of the thermal behavior, an essential factor for the final quality of the cutting tool. In the quality control of the hardmetal, it is also customary to find the values of density, to evaluate the porosity and to check the microstructure, however, it is rare in the literature to determine the thermal diffusivity (α) of the

material manufactured. The thermal diffusivity significance as a thermo-physical measure to be monitored is strongly connected to the material structure. Thus, as thermal diffusivity is the best representative of structural parts, it will depend on the effects of composition and micro-structural variables, as well as materials processing conditions.

The photoacoustic techniques have proved to be a valuable tool to thermal characterization of solids, liquids and gases (Vargas and Miranda, 2003). In this context, the aim of this work was to employ the open photoacoustic cell (OPC) technique to evaluete thermal diffusivity the carbide cutting tool from two different manufacturers. A microstructural characterization by X-ray diffraction and scanning electron microscopy is also presented.

2. MATERIALS AND METHODS

2.1 Sample preparation

The samples used were extracted from two different hardmetal inserts from different manufacturers with the aid of a precision saw, BUEHLER model IsoMet 4000, diamond cutting disc of 15 HC and 4000 rpm. Therefore, the analyzes were performed on the substrate of the inserts, i.e. the inner layer not covered by the coating. The cutting tools manufacturers were omitted and samples named as X and Y. The thickness for the X and Y samples were 505 μm and 655 μm, respectively.

2.2 Open photoacoustic cell technique

The open photoacoustic cell technique (Carvalho, *et al.*, 2013; Dias, *et al.*, 2014; Perondi and Miranda, 1987) consists in a commercial electret's microphone and a solid sample that directly seals the photoacoustic chamber. The sample was fixed using a small amount of *vacuüm* grease on top of an electret microphone. This electret microphone has a non-flat frequency response from 4-150 Hz. Its frequency response was obtained by running a frequency scan of a 102 μm-thick aluminum sample. This sample is thermally thin $(\ell_s a_s << 1)$ up to 10 kHz, and one would expect the photoacoustic (PA) signal dependence on the modulation frequency (*f*) to be $f^{1.5}$ (Perondi and Miranda, 1987). The PA signal depends not only on the amount of heat generated in the sample, but also on how this heat diffuses through the sample. The hardmetal samples were thermally thick and the PA signal obeyed the OPC equation:

$$S = \left(\frac{A}{f}\right) \times exp(-b\sqrt{f}) \tag{1}$$

where the coefficient *A* contains the instrumental transfer function and is independent of the samples thickness, and $b = \sqrt{\pi \ell^2 / \alpha_s}$ the linear adjusting parameter, where: ℓ is the sample thickness; and α_s the sample thermal diffusivity. The thermal diffusivity measures the rate of heat diffusion in the sample and it is defined by:

$$\alpha = \frac{k}{\rho c}, \tag{2}$$

where: *k* is the thermal conductivity; ρ is the density; and *c* is the heat capacity of the sample at a constant pressure.

Depending on the linear thermal expansion coefficient and thickness of the sample, a thermoelastic contribution may appear in thermally thick regime $(\ell_s a_s >> 1)$ (Perondi and Miranda, 1987). If this contribution can be separated out at higher frequencies, as is the case with our photoacoustic experiments, it may be theoretically ignored.

Figure 1 shows the scheme for the thermal diffusivity measurements using the open photoacoustic cell technique. The PA signal was generated by illuminating the samples with a modulated light beam. It was used a 25 mW laser at 637 nm (Coherent) mechanically chopped from (SR540, Stanford Research System) and uniformly focused directly the sample. A Lock-in amplifier (SR530, Stanford Research System) was used to analyze the amplitude of the microphone signal. The signal amplitude and phase were both recorded as a function of the modulation frequency.

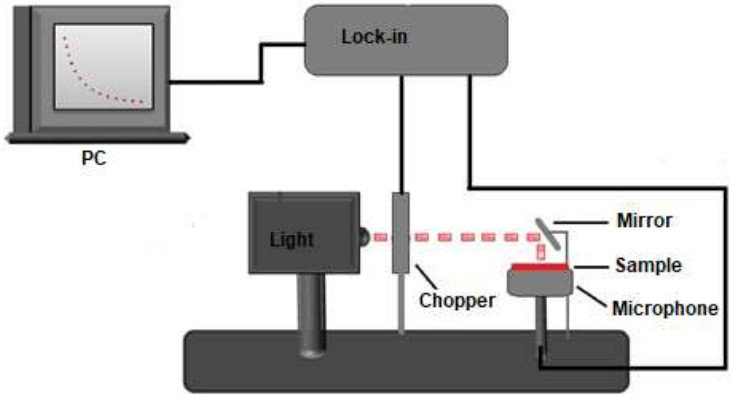

Figure 1. Experimental scheme OPC

2.3 Microstructural characterization

The microstructural characterization of the hardmetal samples was performed with the aid of scanning electron microscope (SEM) of the Shimadzu brand, model SSX – 550 and an X-ray diffractometer from Rigaku – Ultima IV.

For the SEM, the samples were embedded in bakelite with zirconia and copper and polished with sandpaper of 120 and 635 grit, finished with diamond paste. However, due to the limited electrical conductivity of this material, a conductive tape was applied to the embedded samples and gold electrodeposition was applied.

3. RESULTS AND DISCUSSIONS

3.1 Thermal diffusivity and literature comparison

OPC experiments were performed seven times for each side of the sample in ten runs of 20-85 Hz modulation-frequency range. The photoacoustic signal amplitude was normalized by the microphone response function (Carvalho, *et al*., 2013). Figure 2 is a typical semilogarithmic graph of the normalized amplitude as function of the square root of modulation frequency for the sample Y. In the 25-55 Hz frequency range, the signal amplitude is dominated by an exponential behavior, $\sim exp\ (-bf^{1/2})$, as predicted by the thermal diffusion model, for a thermally thick sample (Carvalho, *et al.*, 2013). After fitting the photoacoustic signal and finding the variable b the thermal diffusivity was 28.0×10^{-6} m^2/s.

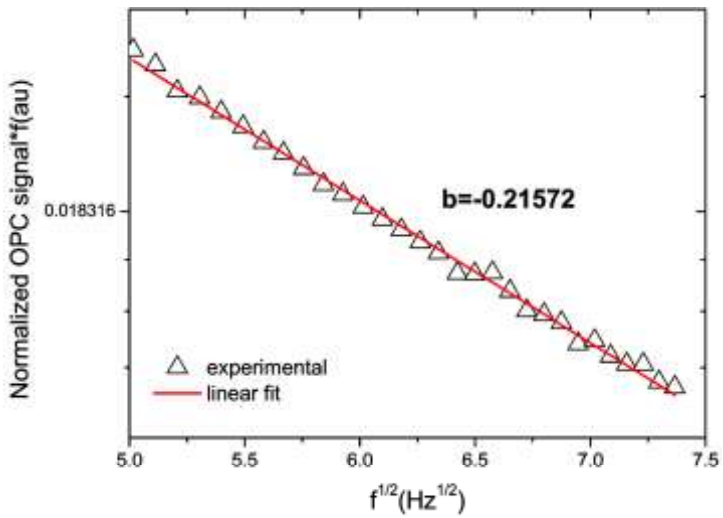

Figure 2. Typical linear plot of normalized OPC signal * *f* as function of the square root of *f*

The Tab. 1 presents the average thermal diffusivity of the samples. The experimental error on the b value was calculated by using the standard formula for error propagation.

Table 1. Average thermal diffusivity. Side A represents the surface layer of the tool and the B deeper layer.

Sample	Thickness (μm)	Side	Average thermal diffusivity ($\times 10^{-6}$ m^2/s)	
X	505	A	18.8 ± 0.7	19.4 ± 0.7
		B	20.0 ± 0.7	
Y	655	A	25.8 ± 0.9	26.3 ± 0.9
		B	26.5 ± 0.9	

The results of Tab. 1 show a subtle difference between the measurements of the two faces evaluated in each insert. This difference was greater for sample x, suggesting a higher homogeneity for sample Y. In addition, there is a difference of 36% in thermal diffusivity between the two commercial tools. Hardmetal works in extreme stress situations, so the higher the thermal diffusivity faster the material achieves thermal equilibrium thus increasing its life. The values found here can be compared to iron (pure) and Steel (AISI 1010), 22.8 $\times 10^{-6}$ m^2/s and 18.8 $\times 10^{-6}$ m^2/s, respectively. Comparisons of the results from the literature are summarized in Tab. 2, for sintered WC-Co samples, via OPC (Machado, *et al.*, 2008; Faria, *et al*., 2005) and via the Flash-Laser method (Miranzo, *et al*., 2002; Li and Baoqi, 1996). However, for the samples of the present paper there is the other materials presence besides the WC-Co, such as TiC, TaC and NbC.

Table 2. Comparison of the thermal diffusivity measurement data from the literature.

Material	Technique	α ($\times 10^{-6}$ m^2/s)	Ref.
Wc-10%wCo Conventional (1450°C/60min/10^{-2}tor)	OPC	45.6 ± 4.1	Machado, *et al.*, 2008
Wc-10%wCo (5GPa/1200°C/1min)		34.0 ± 0.5	
Wc-10%wCo (5GPa/1200°C/2min)		38.0 ± 2.3	
Wc-10%wCo (5GPa/1300°C/1min)		27.0 ± 4.6	
Wc-10%wCo (5GPa/1300°C/2min)		25.0 ± 1.3	
Wc-10%wCo (5GPa/1400°C/1min)		37.0 ± 3.0	
Wc-10%wCo (5GPa/1400°C/2min)		40.0 ± 0.6	
Wc-15%wCo (5GPa/1350°C/2min)	OPC	35	Faria, *et al.*, 2005
Wc-6%wCo	1000°C Flash-Laser	32	Miranzo, *et al.*, 2002
Wc-8%w(Co75%wNi)	Flash-Laser	20.5	Li and Baoqi, 1996

3.2 Microstructural analysis

Figures 3 show the X-ray diffraction pattern for the X and Y hardmetal. A similarity is observed between the two X-ray diffractograms. Peaks related to tungsten carbide (WC), two peaks of dicobalt octacarbonyl ($Co_2(CO)_8$) and two of tungsten trioxide (WO_3) are noted. The first plane phase has not been identified; it may be treated as a solution, i.e. the formation of a non-stable structure resulting from the inserts manufacturing process. The Figs. 3a and 3b suggested that the sintering process didn't promoted new compound formation. On the other hand, the hardmetal Y showed higher intensity of the phases of the three first peaks, $Co_2(CO)_8$ was about 56% higher than for the hardmetal X.

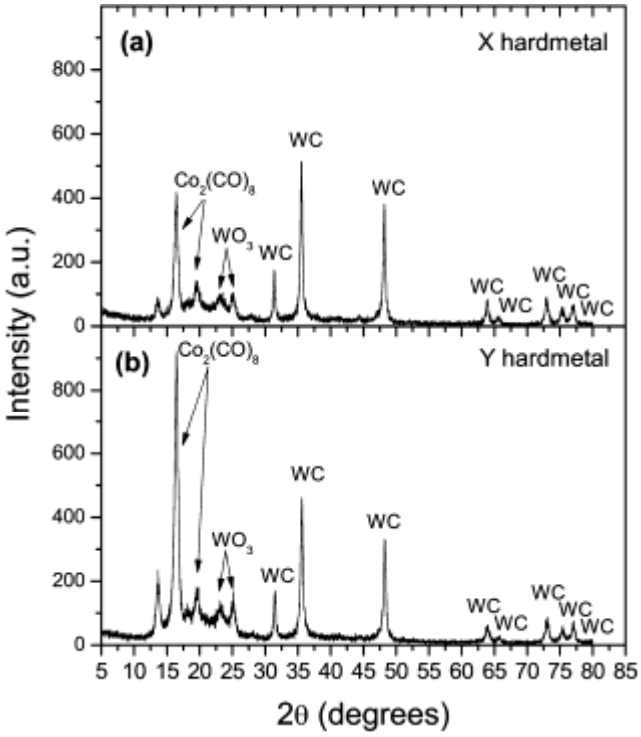

Figure 3. X-ray diffraction pattern of the: (a) X and (b) Y hardmetal

The microstructure of X and Y hardmetal samples is shown in Figs. 4a and 4b, respectively. The typical microstructure of the hardmetal can be observed with the coalescence of some WC particles (light color), homogeneous porosity (black), and distribution of cobalt (dark gray). The Y hardmetal sample showed a more homogeneous microstructure, according to Fig. 4b, which shows a higher distribution of cobalt and lower grain growth. WC grain growth is a common problem in sintering cemented carbide that can affect the mechanical properties (Karimi, *et al*., 2017). The difference in the way these grains are arranged in the entire microstructure is a result of the parameters control of the hardmetal sintering process, i.e., ideal temperature and pressure (Machado, *et al.*, 2008; Karimi, *et al*., 2017). Karimi, *et al*. (2017) studied the high pressure and high temperature sintering of WC-10Co cemented carbide and the hardness, yield strength and compressive strength increase by increasing sintering temperature up to 1700 °C and then decrease. They concluded that the increase at first part is related to improving sintering phenomenon by increasing temperature and the decrease in second part is related to WC particles growth at high sintering temperature.

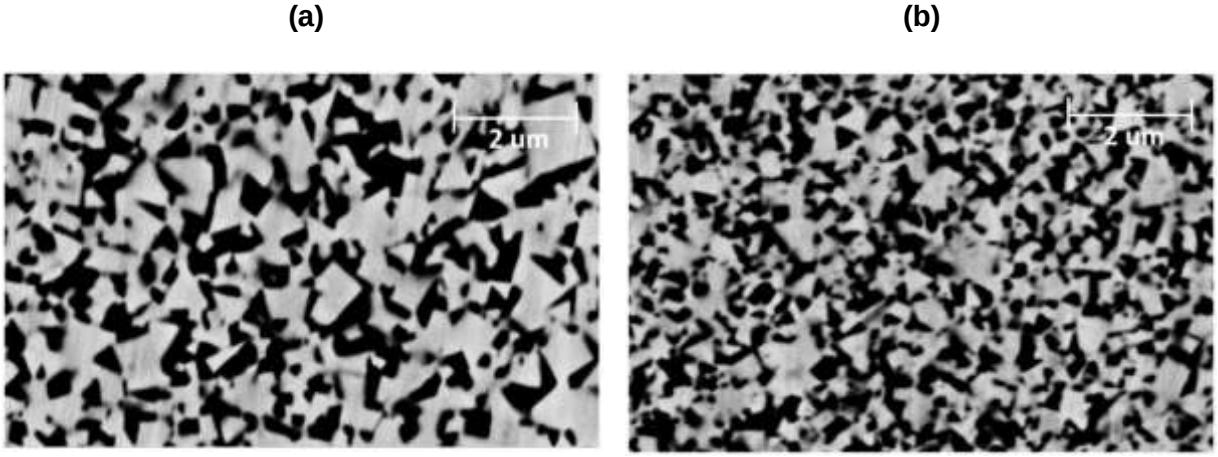

Figure 4. Microstructure of the: (a) X and (b) Y sintered body

The Figs. 3b and 4b, for sample Y, suggest that the higher intensity of the phases $Co_2(CO)_8$ and the more refined microstructure, with little grain growth, respectively, contributed to a thermal diffusivity 36% higher than the value of the manufacturer X. Lauwers, *et al.* (2006) described the influence of composition and grain size of WC-based

cemented on manufacturability by wire-EDM. They found that the cutting rate (mm^2/min), after roughing and under the same machining conditions, decreased with increasing cobalt content due to the high thermal conductivity product and the Co melting point. In addition, it is showed that the cutting rate decreases with increasing WC-grain size, which can be explained mainly by the change in thermal conductivity of the material.

4. CONCLUSIONS

The OPC technique was able to give thermal diffusivity measurements for commercial hardmetal inserts used in the milling process and made it possible to study the way heat is diffused in the samples. The values present results lower than the reference ones, due to low amount of Co. The thermal diffusivity values found for X and Y hardmetal samples were $(19.4 \pm 0.7) \times 10^{-6}$ m^2/s and $(26.3 \pm 0.9) \times 10^{-6}$ m^2/s. Therefore the heat propagation velocity is higher for the Y hardmetal sample. It was observed that the hardmetal of different manufacturers showed similarities in their chemical components. On the other hand, the Y hardmetal sample had a finer microstructure, and little growth of WC-Co grains and so higher thermal diffusivity. In this case, we suggest that the higher thermal diffusivity is desirable to increase the useful life of the tool. Future measurements should be made with respect to cutting rate.

5. ACKNOWLEDGEMENTS

The authors are grateful to FUNTEF-PR, PLN 0028/2011-LOA, and C-LABMU/PROPESP.

6. REFERENCES

Carvalho, A.P.N., *et al.*, 2013. “In vitro thermal diffusivity measurements as aging process study in human tooth hard tissues”. *Journal of Applied Physics*, Vol. 114, p. 194705.

Dias, D.T., *et al.*, 2014. “Photoacoustic spectroscopy and thermal diffusivity measurement on hydrogenated amorphous carbon thin films deposited by plasma-enhanced chemical vapor deposition”. *Diamond & Related Materials*, Vol. 48, p. 1.

Davim, J.P., 2011. *Machining of Hard Materials*. Springer, London.

Faria, T., *et al.*, 2005. “On the thermal characterization of a HPHT sintered WC-15% wt Co hardmetal alloy”. *International Journal of Refractory Metal and Hard Materials*, Vol. 23, p. 115.

Karimi, M.M, *et al.*, 2017. “High pressure assisted WC/Co hardmetal sintering–effect of sintering temperature” *In Proceedings of the 6th Congress and Exhibition on International Advances in Applied Physics and Materials Science – APMAS2016*. Instanbul, Turkey.

Li, Z. and Baoqi, S., 1996. “A new hardmetal for mining with Ni–Co binder”. *International Journal of Refractory Metal and Hard Materials*, Vol. 14, p. 245.

Machado, F.A, *et al.* 2008. “Thermal properties of WC-10 wt. (%) Co Alloys”. *Materials Research*, Vol. 11, n. 1, p. 37.

Miranzo, P., *et al.*, 2002. “Thermal Conductivity enhancement in cutting tools by chemical vapor deposition diamond coating”. *Diamond and Related Materials*, Vol. 11, p. 703.

Myalska, H., *et al.*, 2017. “Effect of nano-sized TiC powder on microstructure and the corrosion resistance of WC-Co thermal spray coatings”. *Surface and Coatings Technology*, Vol. 318, p. 270.

Perondi, L.F. and Miranda, L.C.M., 1987. “Minimal-volume photoacoustic cell measurement of termal diffusivity: Effect of the thermoelastic sample bending”. *Journal of Applied Physics*, Vol. 62, p. 2955.

Su, W., *et al.*, 2016. “Investigation on morphology evolution of coarse grained WC–6Co cemented carbides fabricated by ball milling route and hydrogen reduction route”. International Journal of Refractory Metals and Hard Materials, Vol. 56, p. 110.

Vargas, H. and Miranda L.C.M., 2003. “Photothermal techniques applied to thermophysical properties measurements”. *Review of Scientific Instruments*, Vol. 74, n. 1, p. 794.

7. RESPONSIBILITY NOTICE

The authors are the only responsible for the printed material included in this paper.